

Fig. 4-13 the degraded on-current ratio versus stress time curve of an n-channel ELA TFT without LDD at $V_{DS}=0.1V$

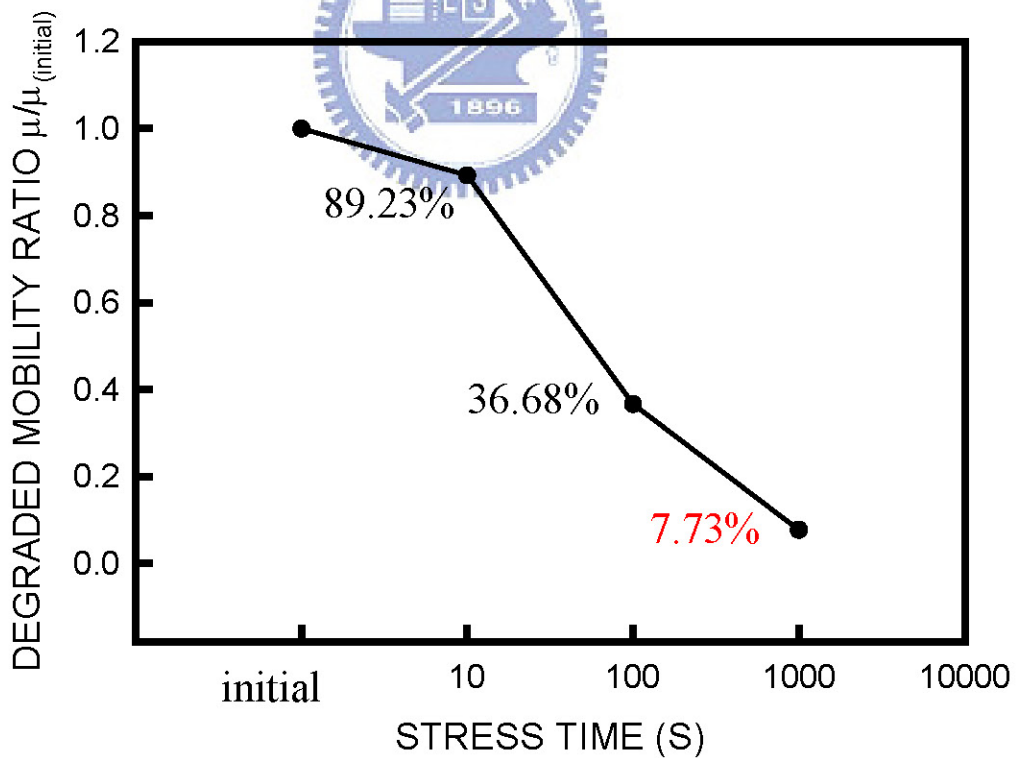


Fig. 4-14 the degraded mobility ratio versus stress time curve of an n-channel ELA TFT without LDD at $V_{DS}=0.1V$

	<i>initial</i>	<i>10s stress</i>	<i>100s stress</i>	<i>1000s stress</i>
<i>POLY-SI TFT WITHOUT LDD</i>	<i>0.611(V/dec)</i>	<i>0.578(V/dec)</i>	<i>0.585(V/dec)</i>	<i>0.662(V/dec)</i>
<i>POLY-SI TFT WITH 1.5 μm LDD</i>	<i>0.592(V/dec)</i>	<i>0.555(V/dec)</i>	<i>0.553(V/dec)</i>	<i>0.567(V/dec)</i>

Table 4-1 the subthreshold swings of poly-Si TFTs without and with LDD after dynamic stress

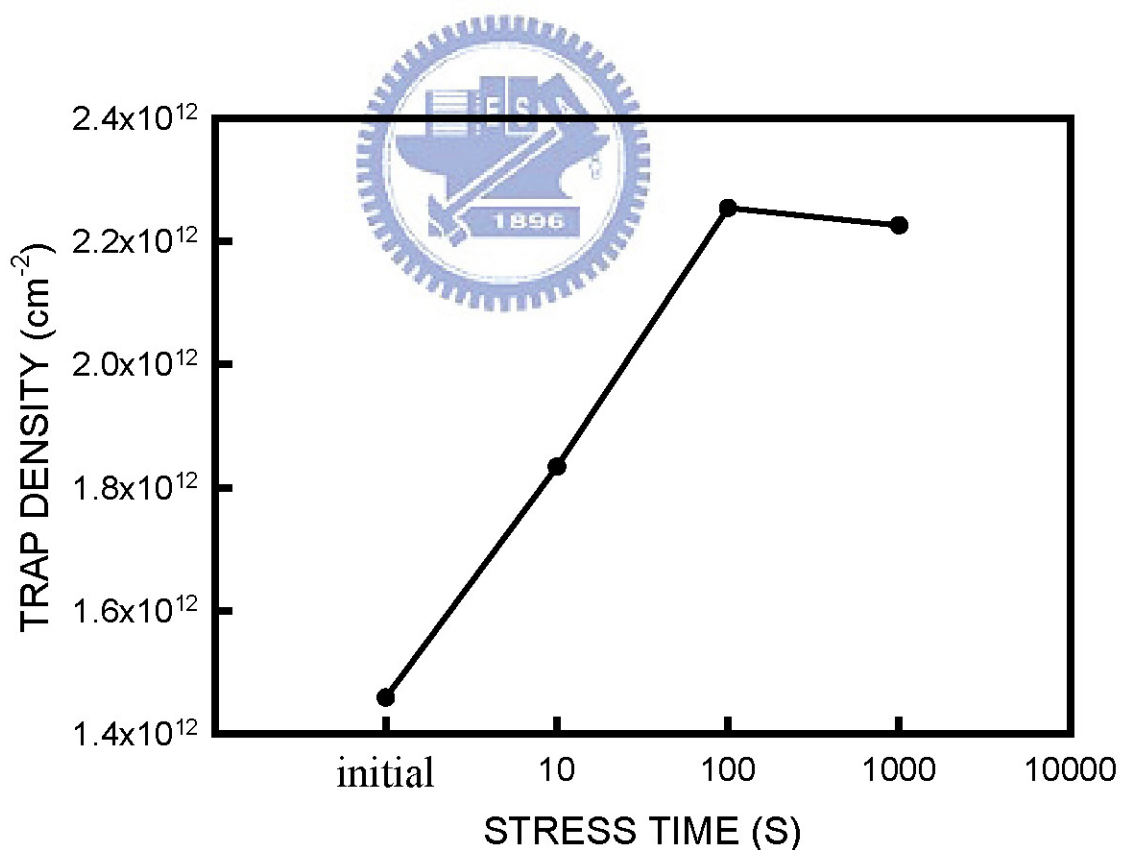


Fig. 4-15 the trap density versus stress time curve of an n-channel ELA TFT without LDD

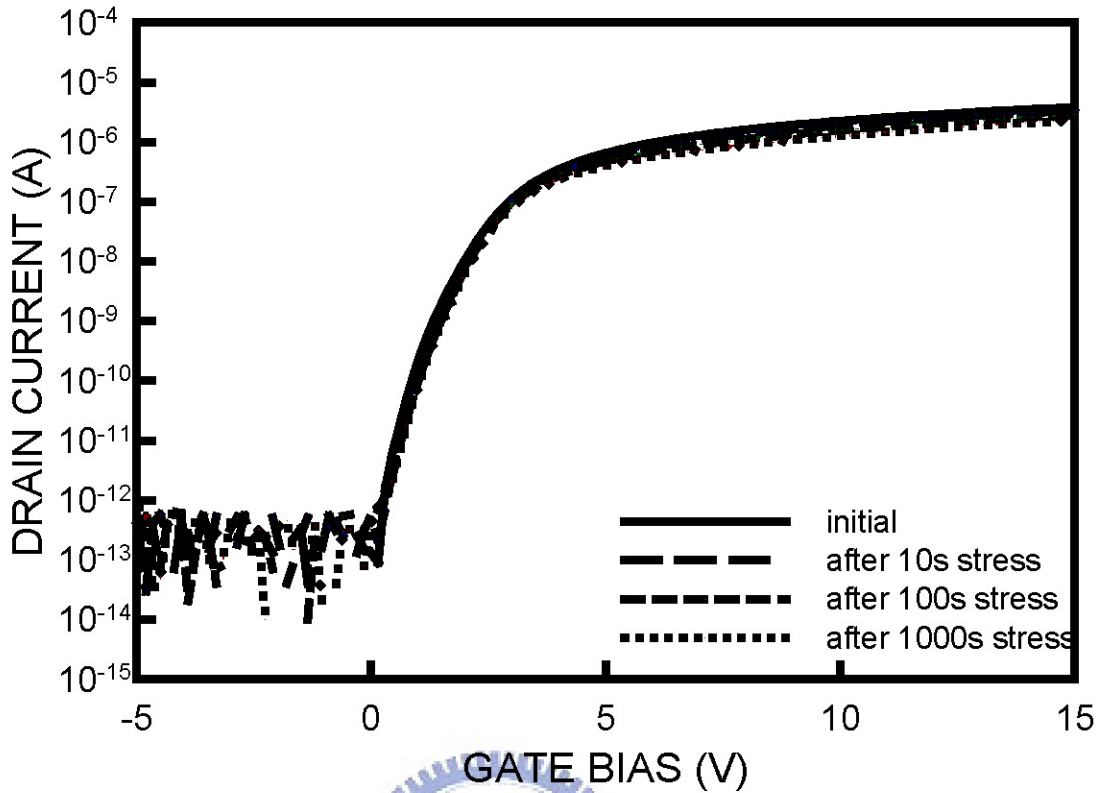


Fig. 4-16 the $I_{DS}-V_{GS}$ curves of an n-channel ELA TFT with $1.5 \mu\text{m}$ LDD at $V_{DS}=0.1\text{V}$

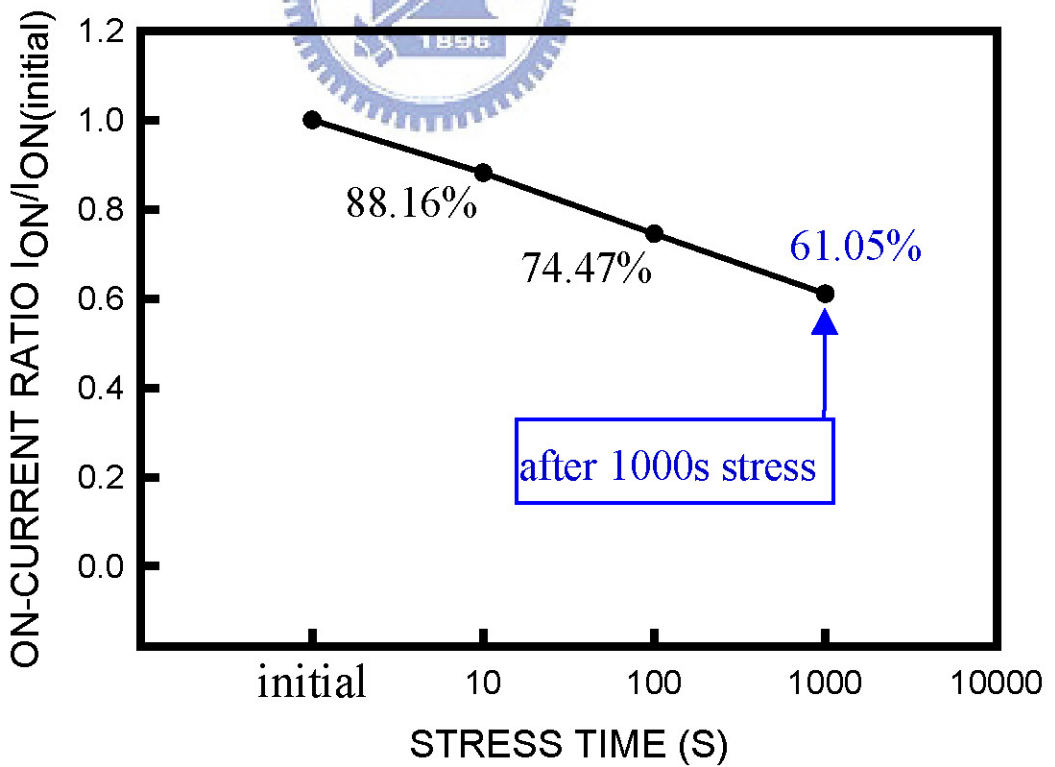


Fig. 4-17 the degraded on-current ratio versus stress time curve of an n-channel ELA TFT with $1.5 \mu\text{m}$ LDD at $V_{DS}=0.1\text{V}$



Fig. 4-18 the degraded mobility ratio versus stress time curve of an n-channel ELA TFT with 1.5 μm LDD at $V_{DS}=0.1\text{V}$

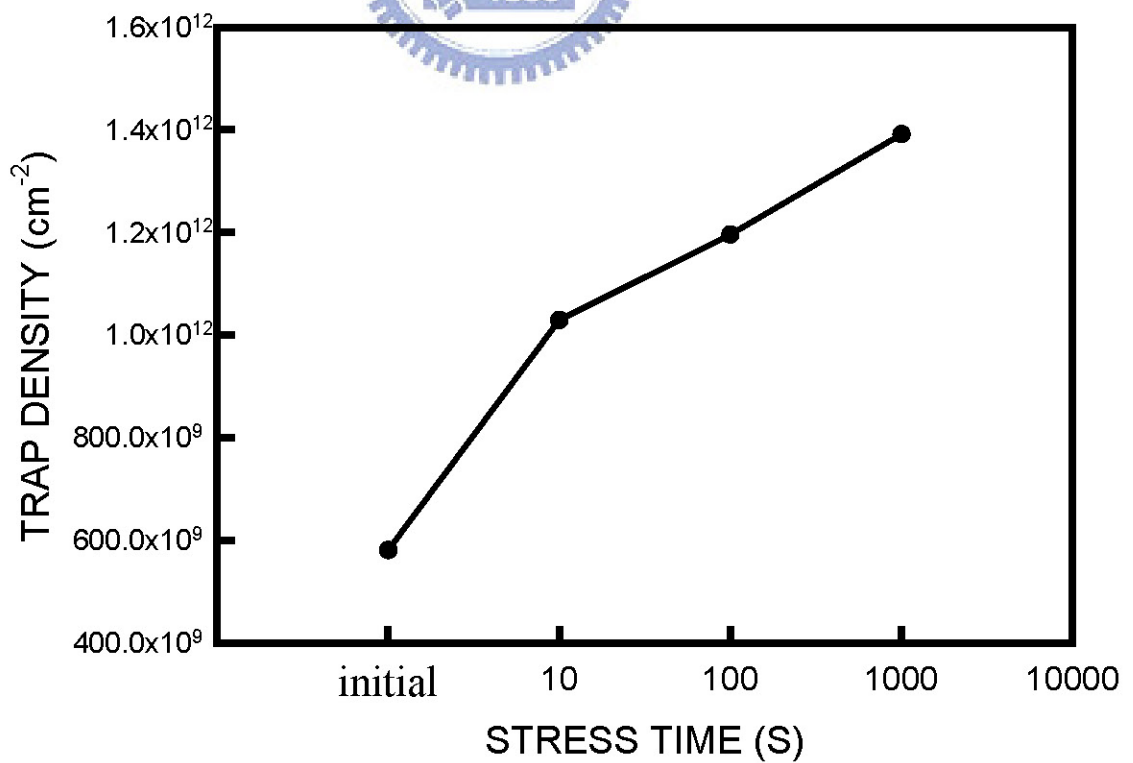


Fig. 4-19 the trap density versus stress time curve of an n-channel ELA TFT with 1.5 μm LDD

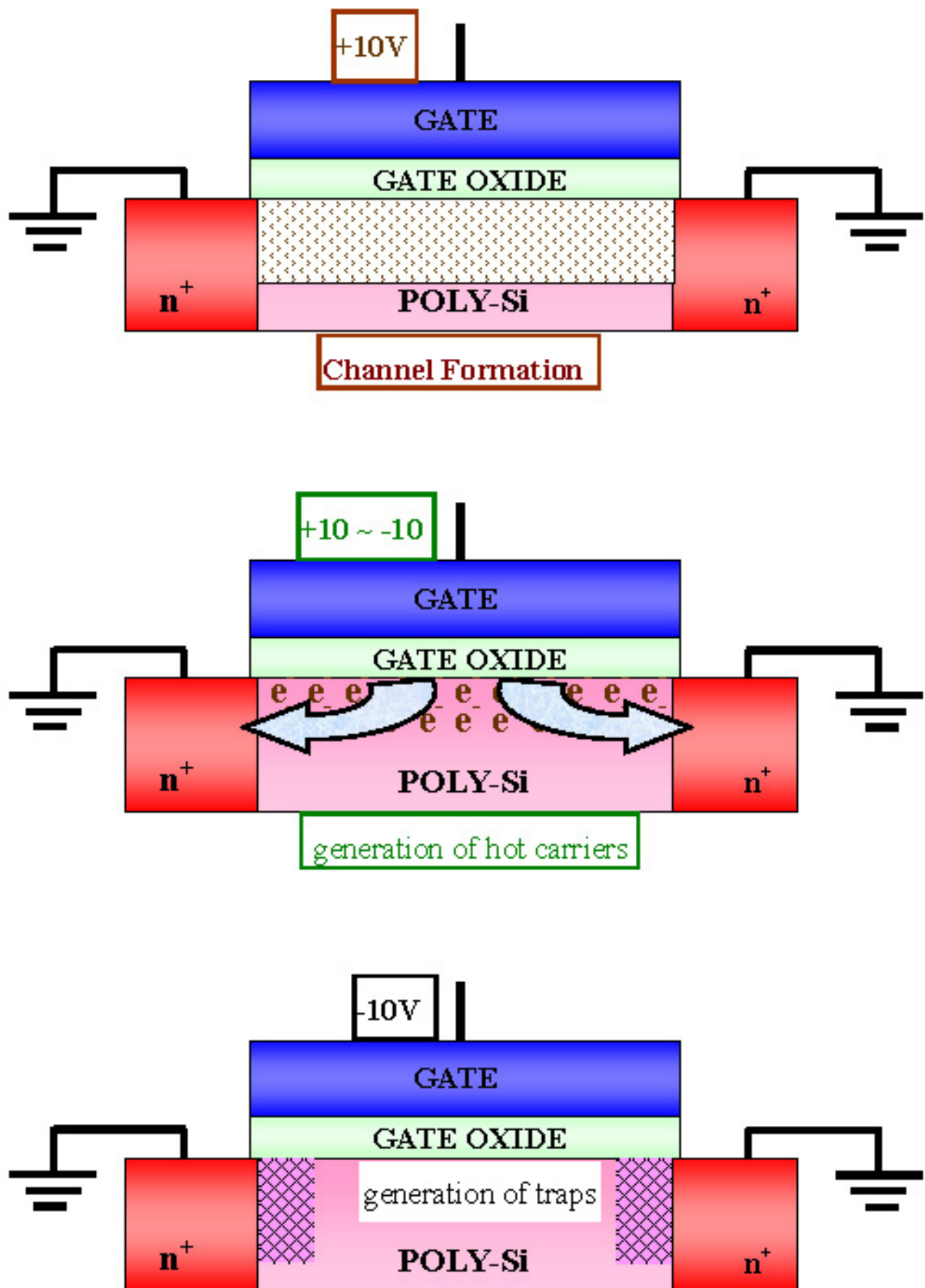


Fig. 4.20 the degradation model under dynamic stress

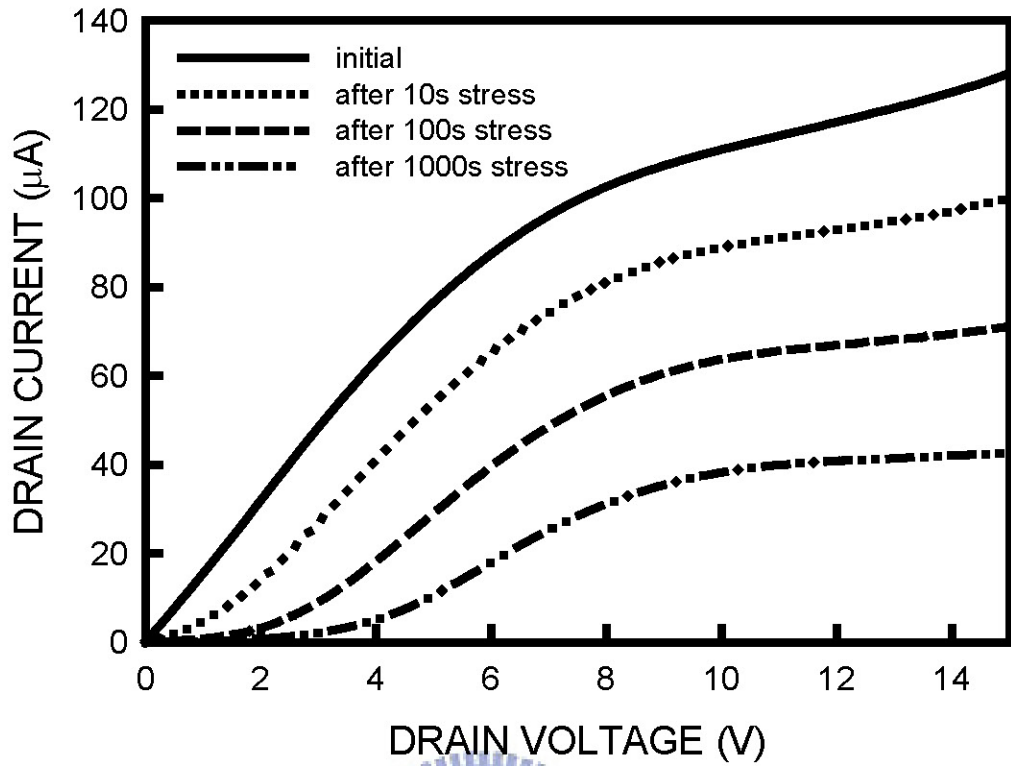


Fig. 4-21 the $I_{DS}-V_{DS}$ curves of an n-channel ELA TFT without LDD at $V_{GS}=10V$

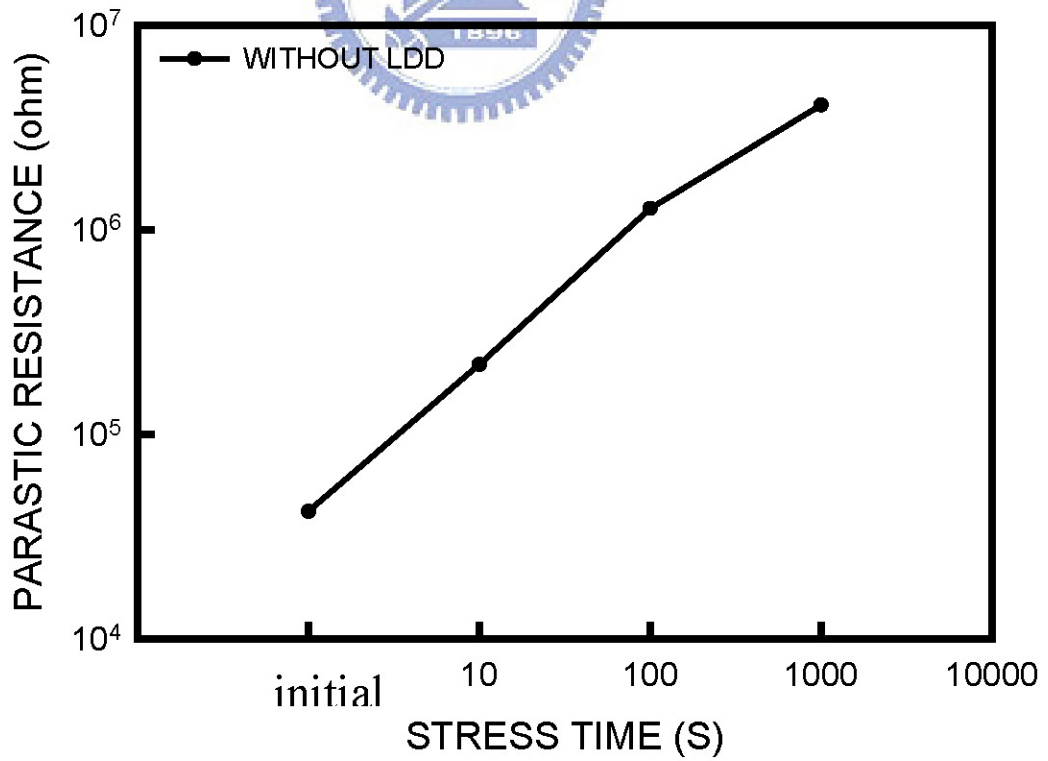


Fig. 4-22 the parasitic resistance versus stress time curve of an n-channel ELA TFT without LDD

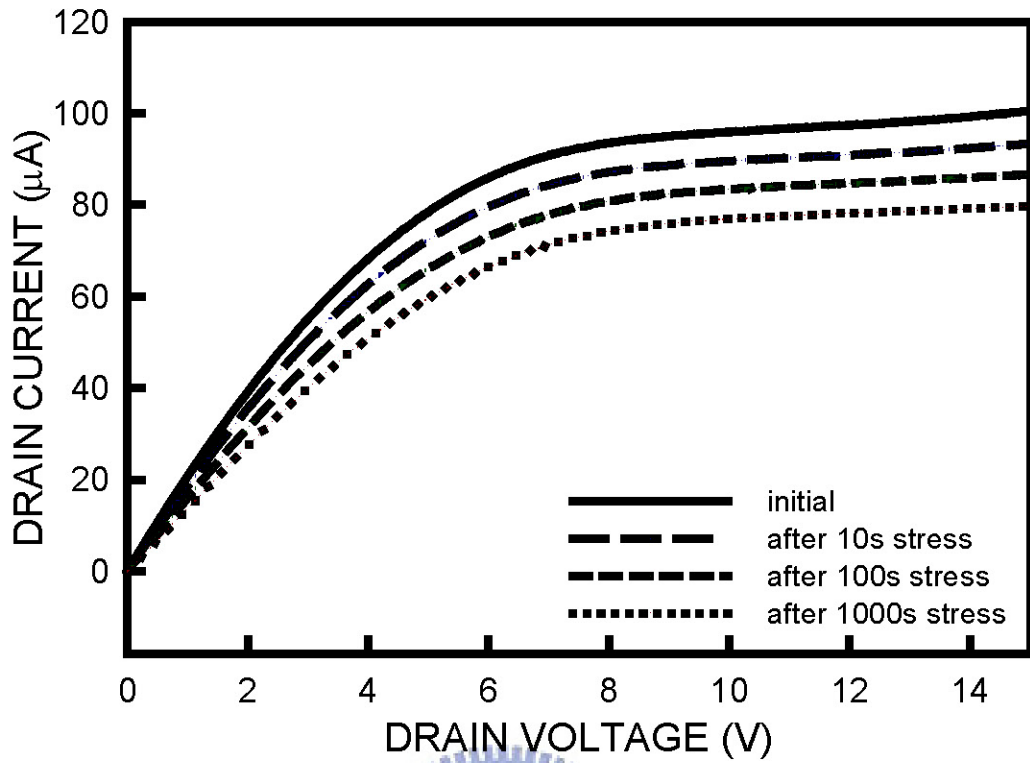


Fig. 4-23 the $I_{DS}-V_{DS}$ curves of an n-channel ELA TFT with $1.5 \mu m$ LDD

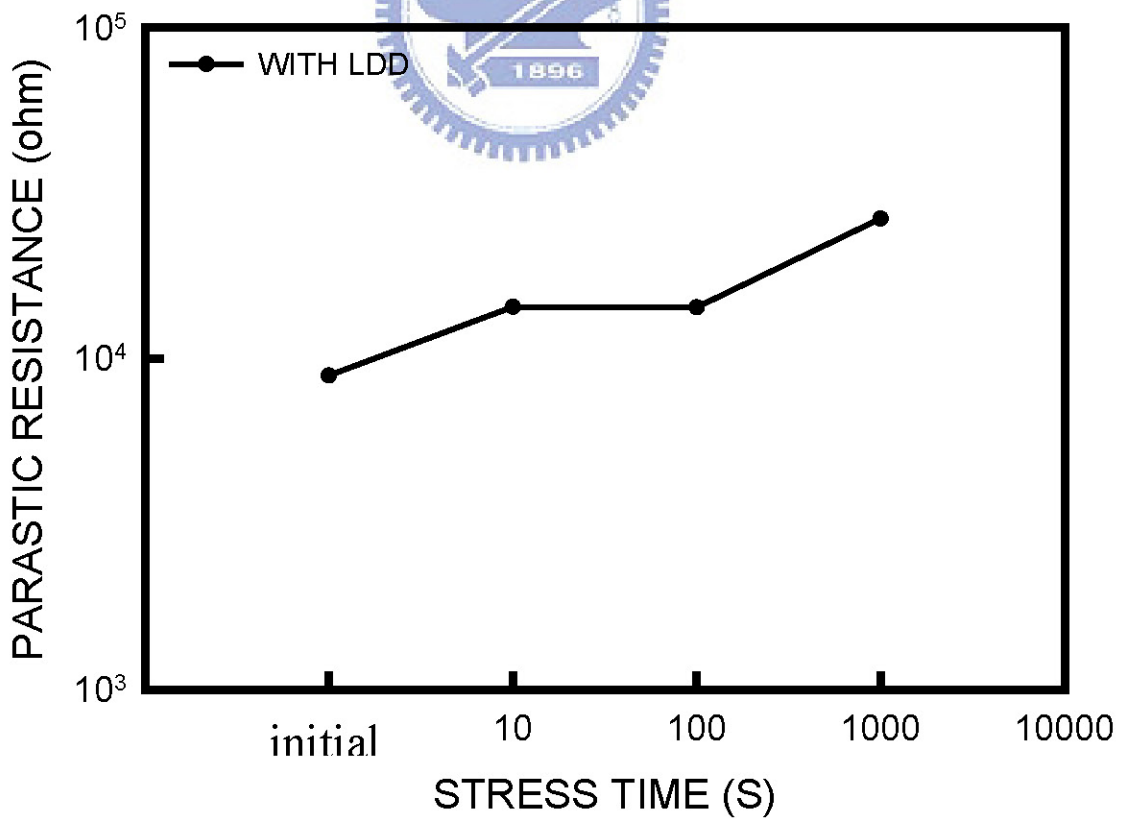


Fig. 4-24 the parasitic resistance versus stress time curve of an n-channel ELA TFT with $1.5 \mu m$ LDD